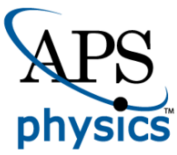

Applicability of the Strongly Constrained and Appropriately Normed Density Functional to Transition-Metal Magnetism

Yuhao Fu and David J. Singh

Phys. Rev. Lett. **121**, 207201 — Published 14 November 2018

DOI: 10.1103/PhysRevLett.121.207201

Applicability of the strongly constrained and appropriately normed density functional to transition metal magnetism

Yuhao Fu[1] and David J. Singh[1,*]

[1] *Department of Physics and Astronomy, University of Missouri, Columbia, MO 65211-7010 USA*

(Dated: October 19, 2018)

We find that the recently developed self consistent and appropriately normed (SCAN) meta-generalized gradient approximation, which has been found to provide highly accurate results for many materials, is, however, not able to describe the stability and properties of phases of Fe important for steel. This is due to an overestimated tendency towards magnetism and exaggeration of magnetic energies, which we also find in other transition metals.

Density functional theory (DFT) calculations[1] are a central tool in condensed matter physics, chemistry, and materials science. This utility is the result of the availability of sufficient accuracy in tractable approximate functionals. This enables predictive calculations of properties of interest and elucidations of underlying mechanisms of physical behavior. Therefore the development of new practical functionals that improve the accuracy, and therefore the range of behaviors and materials that can be studied with DFT calculations, is of great interest.

Steel is arguably the most important industrial material. Annual production exceeds 1.7 billion metric tonnes. Steels are complex materials whose properties are controlled by microstructure. These microstructures are what provides steel with desirable combinations of ductility, toughness and tensile strength. These microstructures come from balances between different phases mainly in the Fe-C phase diagram.[2] While the ground state of Fe is body centered cubic (bcc), an an equilibrium face centered cubic (fcc) phase exists between between 1185 K and 1667 K. Carbon has a much higher solubility in this fcc phase (up to 2.14 wt% and 0.76 wt% at the eutectoid) than in the bcc phase (maximum of 0.022 wt%), leading to an easily accessed eutectoid point in the phase diagram (at 1000 K and 0.77 wt% C). Cooling leads to nanoscale and microscale precipitation of cementite (Fe_3C, a very hard phase), in a bcc Fe matrix, as well as non-equilibrium austenite (fcc Fe with C) and sometimes other phases associated with alloying elements, to form microstructures such as perlite, martensite and bainite. These microstructures, sometimes modified by mechanical deformation steps, are key to the properties of steel. First principles based understanding of steel requires the ability to model these different phases and their relationships, most importantly the relationship between the ground state bcc structure (ferrite) and the fcc structure (austenite).

This has posed ongoing challenges to density functional calculations. Early on it was found that the otherwise highly successful local (spin) density approximation (LDA), cannot describe Fe. In particular, it was shown that the LDA predicts a non-magnetic fcc ground state for Fe, with the ferromagnetic bcc structure lying higher in energy.[3] The LDA does, however, provide an accurate value of the spin magnetization of Fe, when constrained to its experimental bcc structure.

An important step was the development of generalized gradient approximation (GGA) functionals,[4–7] based on knowledge of the behavior of the exchange correlation hole in inhomogeneous electron gasses.[8,9] In addition to correctly predicting the bcc ground state and spin magnetization of Fe,[6,10–14] these GGA functionals greatly improved the energetics of a wide variety of molecules and solids. This was a remarkable achievement, especially considering that these GGA functionals were based on constraints and scaling for the electron gas and not fits to known materials properties.

Therefore, it is very reasonable to assume that functionals that incorporate additional known exact properties of the inhomogeneous electron gas will at least on average improve the description of atoms, molecules and solids. A significant recent development along these lines was the construction of a strongly constrained and appropriately normed (SCAN) functional.[15] This is a semi-local meta-GGA functional. Meta-GGA functionals are more convenient for calculations than hybrid functionals,[16,17] especially in extended systems.

The SCAN functional satisfies exact constraints, including importantly the Lieb-Oxford lower bound for the exchange energy,[18,19] also important for the construction of the earlier GGA functionals, as well as scaling relations.[20] It is also designed to revert to the LDA for the uniform electron gas (a norm) and also uses the hydrogen atom as a norm for the exchange. This is important in regards to self-interaction errors. It is designed to be accurate both for the slowly varying electron gas, and for atoms, which is not possible in GGA functionals.[21]

Tests done to date generally confirm the expectation that SCAN provides highly accurate results for many materials,[15,22–25] as might be expected from the many constraints that it satisfies.[26] However, there is at least one indication that SCAN may not improve the already generally good description of magnetism in some metallic ferromagnets. Isaacs and co-workers[25] reported that the magnetization of Fe, Co and Ni are enhanced by 0.42 μ_B, 0.13 μ_B and 0.1 μ_B, respectively, relative to the widely used GGA functional of Perdew, Burke and Ernzerhof (PBE).[7] They observed that this degrades agreement with experiment for Fe and Ni. Ekholm and coworkers, also performed calculations for Fe, Co and Ni,

and found that the moments were enhanced relative to experiment, which they ascribed to a downshift of the 3d states.[27]

We did calculations with the LDA, the PBE GGA and the SCAN functional using two different methods, specifically the projector augmented wave (PAW) method[28] as implemented in the VASP code,[29] and the all electron general potential linearized augmented planewave (LAPW) method,[30] as implemented in the WIEN2k code.[31] The VASP code includes a self-consistent calculation with the SCAN functional, except that that it relies on PAW potentials constructed for the PBE GGA, which is an approximation. The LAPW method as implemented in WIEN2k is an all electron method that does not rely on pseudopotentials. However, at present, SCAN calculations with this method must be done non-self-consistently, in particular, calculating the energy using the SCAN functional, but based on the density from a semi-local calculation. We used the PBE GGA with the constrained DFT,[32] specifically the fixed spin moment (FSM) procedure,[33–35] to generate the spin densities for calculating the SCAN total energies.

This procedure involves solving the Kohn-Sham equations with a constraint that the integrated spin density (the spin-moment) equal a specified value. This is achieved by imposing the constraint via a difference in spin-up and spin-down Fermi levels, equivalent to a magnetic field operating on spin only.[36] We used dense grids of discrete moments to obtain the plots shown here. This allows us also to calculate the total energy as a function of the constrained moment for ferromagnetic materials, and provides insights into the problems in the treatment of magnetic transition metals with SCAN. We carefully converged the calculations, using large basis sets, and dense convergence tested k-point grids for all materials. We compared the results from the two codes and find very similar results, which supports the different approximations involved. We also did self consistent calculations including spin orbit for the PBE and LDA functionals to quantify the effect of spin orbit, which could not be applied in FSM calculations for the SCAN functional. These show that the effects of spin orbit are small on the scale of the differences between the functionals, and cannot resolve the discrepancies.

The measured saturation magnetizations of Fe, Co and Ni are 2.22 μ_B, 1.72 μ_B and 0.62 μ_B, on a per atom basis.[37,38] These include both spin and orbital contributions. The orbital moments of Fe and Co from x-ray magnetic circular dichroism (XMCD) experiments are 0.09 μ_B and 0.15 μ_B, per atom,[39] while the experimental value for Ni is 0.05 μ_B.[40] Our spin (m_{sp}) and orbital (m_{orb}) moments, at the experimental lattice parameters from LAPW calculations with the PBE functional including spin orbit are m_{sp}=2.22 μ_B and m_{orb}=0.04 μ_B for Fe, m_{sp}=1.62 μ_B and m_{orb}=0.08 μ_B for Co, and m_{sp}=0.63 μ_B and m_{orb}=0.05 μ_B for Ni, i.e. spin moments very close to the experimental values, and orbital moments are small and underestimated for Fe and Co, as in prior

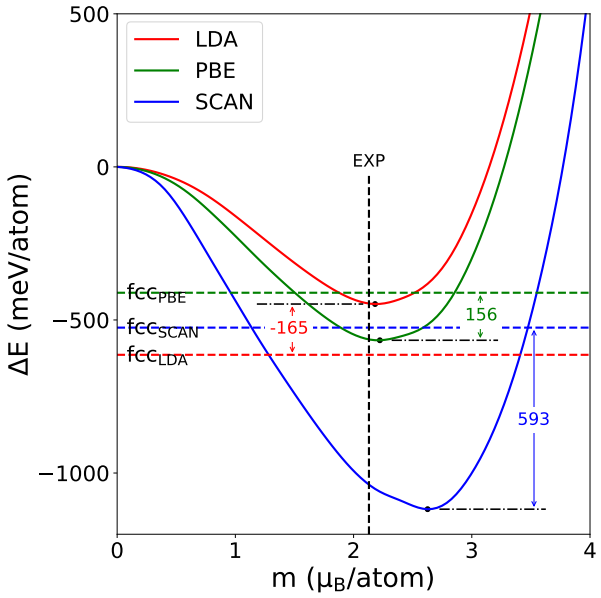

FIG. 1. FSM energy for bcc Fe at the experimental lattice constant of 2.86 Å, on a per atom basis. The dashed lines are the energies of non-spin-polarized fcc Fe, at the optimized lattice parameter for the different functionals. The small dots indicate the minimum energy points.

calculations.[41] In our calculations without spin orbit, the PBE spin moments are m_{sp}=2.22 μ_B, m_{sp}=1.62 μ_B, and m_{sp}=0.63 μ_B, for Fe, Co and Ni, respectively, which are the same as those with spin orbit to the quoted precision. Thus spin orbit does not have a significant effect on the calculated spin moments for these 3d ferromagnets. It is also to be noted that any enhancement of the spin moment over the PBE values will degrade agreement with experiment, including the case of Co.

Fig. 1 shows our results for the magnetic energy of bcc Fe at its experimental lattice parameter, in comparison with the energy of non-spin-polarized fcc Fe. Numerical values and magnetic moments are given in Table I. As seen, the SCAN functional yields dramatically different results from the LDA and PBE functionals. Energy plays a central role in density functional theory. As mentioned, the LDA fails for Fe, predicting that the fcc structure has lower energy, in particular by 0.165 eV. The PBE functional yields the correct ordering, with an energy difference of 0.156 eV, considering a non-magnetic fcc structure. The SCAN functional predicts a much more stable bcc structure, with an overestimated spin moment of 2.63 μ_B/atom and an fcc - bcc energy difference of 0.593 eV. This is due to a much larger magnetic energy. Self consistent calculations using VASP yield similar numbers, specifically a spin moment of 2.65 μ_B and an energy difference of 0.579 eV, for SCAN. While these numbers do not include the magnetic enthalpy of fcc Fe, it is clear that SCAN predicts an overly stable ferromagnetic state for bcc Fe. The experimental enthalpy difference between

TABLE I. Calculated properties of Fe. a_{exp} and a_{calc} are the experimental and calculated lattice parameters of bcc Fe, respectively. The fcc-bcc energy difference $\Delta E_{fcc-bcc}$ is as in Fig. 1. ΔE_{mag} is the magnetic energy from the difference between non-spin polarized and ferromagnetic states. Energies are per atom.

	LDA	PBE	SCAN	Expt.
a (Å)	2.76	2.84	2.85	2.86
$m_{sp}(a_{exp})$ (μ_B)	2.21	2.21	2.63	2.13
$m_{sp}(a_{calc})$ (μ_B)	2.00	2.16	2.60	-
$m_{orb}(a_{exp})$ (μ_B)	0.05	0.04	-	0.09
$\Delta E_{mag}(a_{exp})$ (meV)	448	566	1117	-
$\Delta E_{mag}(a_{calc})$ (meV)	317	529	1078	-
$\Delta E_{fcc-bcc}$ (meV)	-165	156	593	60[a]

[a]estimate from extrapolated thermodynamic data (see text).

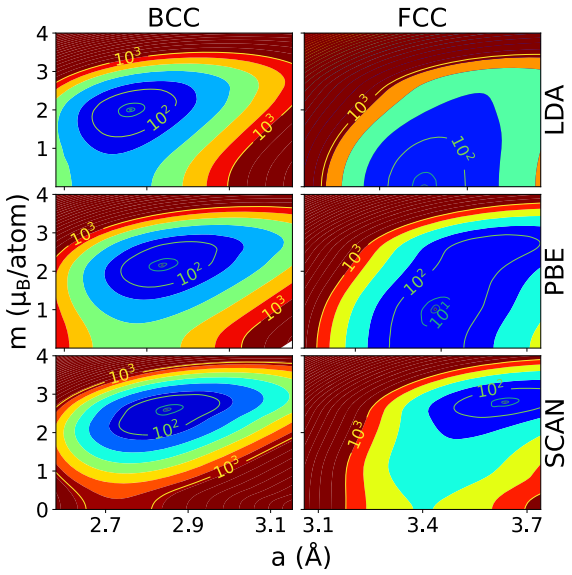

FIG. 2. LDA, PBE and SCAN FSM energy in meV/atom for bcc and fcc Fe as functions of lattice parameter and spin moment.

bcc and fcc Fe at 1185 K from assessed calorimetric measurements is 0.009 eV/atom, while the low temperature energy difference from thermodynamic models based on experimental data is 0.06 eV/atom.[42]

Fig. 2 shows the FSM energy as functions of lattice parameter and moment for bcc and fcc Fe. In accord with older work,[3,14] in addition to its failure to predict the correct ground state, the LDA strongly underestimates the lattice parameter of magnetic bcc Fe, while the PBE GGA give values in closer agreement with experimental data. The SCAN functional gives a lattice parameter similar to PBE for the bcc structure. The SCAN functional predicts very different behavior for the fcc phase. When constrained to ferromagnetism, the LDA and PBE predict either no magnetism or a low moment state. The SCAN functional predicts a high moment state. While high moment ferromagnetism does not preclude a still lower energy ground state with antiferromagnetism, it is incompatible with a weak low moment antiferromagnetic state, due to the large magnetic energy associated with the high moment state.

TABLE II. Magnetic data for Ni and Co from fixed spin moment calculations at the experimental lattice parameters. All quantities are per atom.

		LDA	PBE	SCAN	Expt.
Co	m_{sp} (μ_B)	1.61	1.62	1.79	1.57
	m_{orb} (μ_B)	0.08	0.08	-	0.15
	ΔE_{mag} (meV)	199	255	574	-
Ni	m_{sp} (μ_B)	0.62	0.63	0.76	0.57
	m_{orb} (μ_B)	0.05	0.05	-	0.05
	ΔE_{mag} (meV)	50	61	129	-

Experimental information on the magnetism of free fcc Fe is limited by the fact that it is not a stable low temperature phase. However, fcc Fe films grown epitaxially on Cu are paramagnetic at ambient temperature, and become antiferromagnetic at low temperature with T_N∼65 K,[43] similar to the behavior of small fcc Fe precipitates in an fcc Cu matrix.[44] According to neutron diffraction measurements these have a small moment of ∼0.5μ_B per Fe.[45] Based on this, on this, as well as the properties of non-ferromagnetic austenitic steels,[44] thermodynamic modeling, and extrapolation of alloy data[42,46] it is thought that fcc Fe is an itinerant weak antiferromagnet with a Neel temperature below 70 K, and a relatively small contribution of magnetism to the energy. DFT studies have indicted that there is an additional high volume high spin ferromagnetic state with higher energy, and this has been discussed in connection with the stability of the fcc phase between 1185 K and 1667 K.[14,42]

We also did self consistent calculations with VASP for the energy and moments of a hypothetical antiferromagnetic bcc Fe, where the moments of the two Fe atoms in the conventional cubic cell are oppositely aligned. We find that with the PBE functional the moments as measured by the spin density around Fe sites, is reduced from 2.25 μ_B in ferromagnetic case (note there is a small negative interstitial spin moment of ∼ -0.03 μ_B) to 1.71 μ_B. In contrast, the SCAN result for the antiferromagnetic case of 2.66 μ_B is almost exactly the same as for the ferromagnetic case, i.e. 2.65 μ_B. PBE predicts intermediate itinerant / local moment behavior for bcc Fe, while SCAN predicts that Fe is in the local moment limit, in general disagreement with experiment.[47]

Thus the known data is consistent with good agreement between the predictions of the PBE functional and experiment. Importantly, it is inconsistent with the predictions of the SCAN functional. Specifically, the results point to severe problems in the SCAN predictions for magnetic energies and moments in Fe. It is notable that the differences in magnetic energies between SCAN and the LDA and PBE functionals are much larger than the differences between predictions of those two functionals.

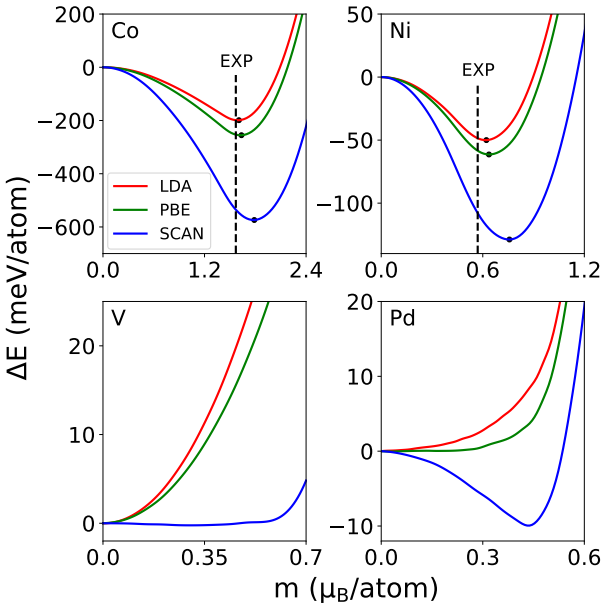

FIG. 3. FSM calculations of the magnetic energy of transition metal elements with the LDA, PBE and SCAN functionals.

Considering the very different predictions of SCAN as compared to standard functionals for the magnetic properties of Fe, it is of interest to investigate whether this is general problem, or if it is restricted to Fe. Accordingly, we performed fixed spin moment and self-consistent calculations for other materials. We start with cementite (Fe_3C), which is ferromagnetic and a key ingredient in many steels. The calculated spin magnetization per three iron atom formula unit is 5.75 μ_B with the PBE functional and 6.87 μ_B with SCAN (based on self-consistent VASP calculations at the experimental lattice parameters; very similar values were obtained from LAPW FSM calculations). This compares with a total room temperature saturation magnetization of 5.3 μ_B from experiment,[48] indicating again a substantial error with SCAN.

Fig. 3 and Table II give the results of FSM calculations for other elements with the experimental structures and lattice parameters. Hexagonal close packed (hcp) Co and fcc Ni are the other ferromagnetic 3d elements. Ni is regarded as a prototypical itinerant ferromagnet. SCAN gives very much larger magnetic energies for these two elements as compared with PBE and LDA. We also find enhanced spin moments with SCAN, and similar to Fe we find significant degradation with respect to experiment for both Ni and Co. The calculated spin moments with the SCAN functional are 1.80 μ_B for Co and 0.77 μ_B for Ni. bcc V and fcc Pd are both paramagnetic metals down to 0 K according to experiment. Pd is very close to ferromagnetism, and for this reason exhibits strong spin fluctuations that have been implicated in preventing a superconducting state in this element.[49,50] Pd is a particularly interesting test for density functionals, since it is incorrectly predicted to be ferromagnetic by some hybrid functionals,[51] while showing borderline ferromagnetic behavior with standard GGAs.[51,52] V is not as close to ferromagnetism and is a superconductor at low temperature.[53] Our PBE and LDA results are consistent with these experimental facts. SCAN on the other hand predicts an effectively infinite susceptibility for V, and a low moment ferromagnetic state for Pd. Thus qualitatively similar to Fe, SCAN strongly overestimates the magnetic tendencies of V, Co, Ni and Pd.

The above results point to a surprising degradation of the predictions of SCAN relative to PBE in describing magnetism in transition metals, and suggest caution in the use of this functional for predicting magnetic properties of materials. This may perhaps be due to the challenge of obtaining the itinerant physics of systems like Fe with multiple partially occupied d-orbitals, and at the same time reproducing correct physics of atoms, including cancellation of self-interaction. In any case, we hope that the above results may motivate further work to develop improved meta-GGA functionals, particularly functionals that satisfy known constraints, from the inhomogeneous electron gas, including the many constraints satisfied by SCAN, and possibly additional constraints, and at the same time predict accurate magnetic properties of metals.

This work was supported by the U.S. Department of Energy, Office of Science, Basic Energy Sciences, Award Number DE-SC0019114. We are grateful for helpful discussions with Guangzong Xing.

* singhdj@missouri.edu

[1] W. Kohn and L. J. Sham, Phys. Rev. **140**, A1133 (1965).
[2] B. L. Bramfitt, in *Metals Handbook, Desk Edition, 2nd. Ed.*, edited by J. R. Davis (ASM International, Materials Park, 1998) pp. 153–173.
[3] C. S. Wang, B. M. Klein, and H. Krakauer, Phys. Rev. Lett. **54**, 1852 (1985).
[4] D. C. Langreth and M. J. Mehl, Phys. Rev. B **28**, 1809 (1983).
[5] J. P. Perdew, Phys. Rev. B **33**, 8822 (1986).
[6] J. P. Perdew, J. A. Chevary, S. H. Vosko, K. A. Jackson, M. R. Pederson, D. J. Singh, and C. Fiolhais, Phys. Rev. B **46**, 6671 (1992).
[7] J. P. Perdew, K. Burke, and M. Ernzerhof, Phys. Rev. Lett. **77**, 3865 (1996).
[8] O. Gunnarsson and B. I. Lundqvist, Phys. Rev. B **13**, 4274 (1976).
[9] R. O. Jones and O. Gunnarsson, Rev. Mod. Phys. **61**, 689 (1989).
[10] D. J. Singh, W. E. Pickett, and H. Krakauer, Phys. Rev.

B **43**, 11628 (1991).
[11] C. Amador, W. R. L. Lambrecht, and B. Segall, Phys. Rev. B **46**, 1870 (1992).
[12] J. Zhu, X. W. Wang, and S. G. Louie, Phys. Rev. B **45**, 8887 (1992).
[13] T. Asada and K. Terakura, Phys. Rev. B **46**, 13599 (1992).
[14] J. Haglund, Phys. Rev. B **47**, 566 (1993).
[15] J. Sun, A. Ruzsinszky, and J. P. Perdew, Phys. Rev. Lett. **115**, 036402 (2015).
[16] A. D. Becke, J. Chem. Phys. **98**, 5648 (1993).
[17] J. Heyd, G. E. Scuseria, and M. Ernzerhof, J. Chem. Phys. **124**, 219906 (2006).
[18] J. P. Perdew, A. Ruzsinszky, J. Sun, and K. Burke, J. Chem. Phys. **140**, 18A533 (2014).
[19] E. H. Lieb and S. Oxford, Int. J. Quant. Chem. **19**, 427 (1981).
[20] M. Levy, Phys. Rev. A **43**, 4637 (1991).
[21] J. P. Perdew, A. Ruzsinszky, G. I. Csonka, O. A. Vydrov, G. E. Scuseria, L. A. Constantin, X. Zhou, and K. Burke, Phys. Rev. Lett. **100**, 136406 (2008).
[22] J. Sun, R. C. Remsing, Y. Zhang, Z. Sun, A. Ruzzinszky, H. Peng, Z. Yang, A. Paul, U. Waghmare, X. Wu, M. L. Klein, and J. P. Perdew, Nature Chemistry **8**, 831 (2016).
[23] F. Tran, J. Stelzl, and P. Blaha, J. Chem. Phys. **144**, 204120 (2016).
[24] Y. Zhang, D. A. Kitchaev, J. Yang, T. Chen, S. T. Dacek, R. A. Samiento-Perez, M. A. L. Marques, H. Peng, G. Ceder, J. P. Perdew, and J. Sun, npj Comput. Mater. **4**, 9 (2018).
[25] E. B. Isaacs and C. Wolverton, Phys. Rev. Mater. **2**, 063801 (2018).
[26] R. Singh and M. K. Harbola, J. Chem. Phys. **147**, 144105 (2017).
[27] M. Ekholm, D. Gambino, H. J. M. Jonsson, F. Tasnadi, B. Alling, and I. A. Abrikosov, Phys. Rev. B **98**, 094413 (2018).
[28] G. Kresse and D. Joubert, Phys. Rev. B **59**, 1758 (1999).
[29] G. Kresse and J. Furthmüller, Phys. Rev. B **54**, 11169 (1996).
[30] D. J. Singh and L. Nordstrom, *Planewaves, Pseudopotentials, and the LAPW method, 2nd Ed.* (Springer, Berlin, 2006).
[31] P. Blaha, K. Schwarz, G. K. H. Madsen, D. Kvasnicka, and J. Luitz, WIEN2k, An augmented plane wave+ local orbitals program for calculating crystal properties (2001).
[32] P. H. Dederichs, S. Blugel, R. Zeller, and H. Akai, Phys. Rev. Lett. **53**, 2512 (1984).
[33] K. Schwarz and P. Mohn, J. Phys. F **14**, L129 (1984).
[34] V. L. Moruzzi, P. M. Marcus, K. Schwarz, and P. Mohn, Phys. Rev. B **34**, 1784 (1986).
[35] V. L. Moruzzi, Phys. Rev. Lett. **57**, 2211 (1986).
[36] D. Wagner, J. Phys.: Condens. Matter **1**, 4635 (1989).
[37] H. Danan, A. Herr, and A. J. P. Meyer, J. Appl. Phys. **39**, 669 (1968).
[38] H. P. Meyers and W. Sucksmith, Proc. Roy. Soc. A **207**, 427 (1951).
[39] C. T. Chen, Y. U. Idzerda, H. J. Lin, N. V. Smith, G. Meigs, E. Chaban, G. H. Ho, E. Pellegrin, and F. Sette, Phys. Rev. Lett. **75**, 152 (1995).
[40] M. B. Stearns, in *Landolt-Börnstein - New Series, Group III, Vol. 19A*, edited by H. P. J. Wijn (Springer Verlag, Berlin, 1986).
[41] G. H. O. Daalderop, P. J. Kelly, and M. F. H. Schuurmans, Phys. Rev. B **41**, 11919 (1990).
[42] Q. Chen and B. Sundman, J. Phase Equilibria **22**, 631 (2001).
[43] W. A. A. Macedo and W. Keune, Phys. Rev. Lett. **61**, 475 (1988).
[44] U. Gonser, C. J. Meechan, A. H. Muir, and H. Wiedersich, J. Appl. Phys. **34**, 2373 (1963).
[45] Y. Tsunoda, J. Phys.: Condens. Matter **1**, 10427 (1989).
[46] M. Acet, H. Zahres, E. F. Wassermann, and W. Pepperhoff, Phys. Rev. B **49**, 6012 (1994).
[47] V. Heine, J. H. Samson, and C. M. M. Nex, J. Phys. F **11**, 2645 (1981).
[48] L. J. E. Hofer and E. M. Cohn, J. Am. Chem. Soc. **81**, 1576 (1959).
[49] N. F. Berk and J. R. Schrieffer, Phys. Rev. Lett. **17**, 433 (1966).
[50] P. Larson, I. I. Mazin, and D. J. Singh, Phys. Rev. B **69**, 064429 (2004).
[51] F. Tran, D. Koller, and P. Blaha, Phys. Rev. B **86**, 134406 (2012).
[52] D. J. Singh and J. Ashkenazi, Phys. Rev. B **46**, 11570 (1992).
[53] B. W. Roberts, J. Phys. Chem. Ref. Data **5**, 581 (1976).